ECRONICON OPEN ACCESS

EC NEUROLOGY
Research Article

MRI Features of Brain and Spine in Patients Series with Mucopolysaccharidosis

Khadija Laasri[1]*, Abderrazzak Ajertil[2], Manal Jidal[1], Siham El Haddad[1], Nazik Allali[1], Abdeljalil El Quassar[2] and Latifa Chat[1]

[1]Pediatric Radiology Department, Children's Hospital, Ibn Sina Hospital, Mohamed V University, Rabat, Morocco

[2]Radiology Department, Cheikh Zaid's Hospital, International University Hospital, Rabat, Morocco

***Corresponding Author:** Khadija Laasri, Pediatric Radiology Department, Children's Hospital, Ibn Sina Hospital, Mohamed V University, Rabat, Morocco.

Received: March 09, 2023; **Published:** March 15, 2023

Abstract

Background: Mucopolysaccharidosis represent a group of rare hereditary disorders characterized by multisystem involvement due to intralysosomal glycosaminoglycans accumulation. Central and peripheral nervous systems are both affected by almost all types of disease among various tissue. Therefore, brain and spinal MRI are valuable tools for assessing neurologic involvement, and there is evidence that they may be accurate indicators of disease severity and the efficacy of current treatment options in patients with MPS.

Aim: To describe the magnetic resonance imaging findings of the brain and spine in patients with mucopolysaccharidosis and correlate them with the type of MPS and clinical severity, and finally to compare these findings with those previously reported.

Materials and Methods: Retrospective evaluation was conducted of brain and spine MRI of 12 patients diagnosed with MPS from 2021 to this day, of these patients, 8 had type I (6 with Hurler syndrome and 2 with Hurler-Scheie syndrome), 2 had type II or Hunter syndrome (1 with the severe form and 1 with the mild form), 1 had type III or Sanfilippo syndrome and 1 had type VI or Maroteaux-Lamy syndrome.

Results: We enrolled 12 patients affected by MSP (07 females and 06 males, age range 5 - 14 years at the time of MRI). We observed a wide spectrum of MRI anomalies. In brain MRI: perivascular space enlargements (n = 08/12; 20%), white matter signal alterations (n = 06/12; 15%), ventriculomegaly/hydrocephalus (n = 05/12; 12%), Cortical and subcortical cerebral atrophy (n = 04/12; 10%), Posterior fossa abnormalities (n = 04/12; 10%), arachnoid cyst (n = 04/12; 10%), closed meningo-encephalocele (n = 02/12; 5%), bilateral optic nerve sheaths enlargement (n = 02/12; 5%), craniosynostosis (scaphocephaly: n = 04/12; 10%), morphological abnormality of sella turcica (n = 01/12; 3%). In spine MRI: periodontoid soft-tissue thickening (n = 07/12; 20%), spinal canal stenosis (n = 07/12; 20%), cord compression (n = 04/12; 11%), myelopathy (n = 02/12; 6%), syringomyelia (n = 02/12; 6%), Odontoid hypoplasia (n = 03/12; 8%), morphological abnormality of vertebral bodies (n = 07/12; 20%), kyphosis (n = 02/12; 6%), scoliosis (n = 01/12; 3%).

Conclusion: The spectrum of brain and spinal MRI abnormalities in MPS is extremely broad (Perivascular space enlargements, white matter signal alterations, ventriculomegaly/hydrocephalus, cerebral atrophy, periodontoid soft-tissue thickening, spinal canal stenosis; with/or without cord compression or myelopathy, vertebral/skull abnormalities). Therefore, given these abnormalities, we should be aware of this possible diagnosis, especially when typical signs and symptoms are present. However, we did not find a correlation between these findings and either any specific type of MPS or clinical severity.

Keywords: *Mucopolysaccharidosis; Glycosaminoglycans; Magnetic Resonance Imaging; Brain; Spine*

Abbreviations

MSP: Mucopolysaccharidosis; MRI: Magnetic Resonance Imaging; GAGs: Glycosaminoglycans; PVSE: Perivascular Space Enlargement; WMSAs: White Matter Signal Alterations; CSF: Cerebrospinal Fluid; CNS: Central Nervous System

Introduction

MSP are a heterogeneous group of inherited rare metabolic lysosomal storage disorders characterized by defective degradation of long-chain complex carbohydrate, called glycosaminoglycans (GAGs) (previously known as mucopolysaccharides) [1], leading to accumulation of these partially degraded macromolecules within lysosomes and in the extracellular space, culminating in cell dysfunction of several organs and body tissues [1]. According to the deficient lysosomal enzyme, there are currently 7 distinct types of MPS that have been identified, which are divided further into subtypes according to the deficient enzyme and severity of the clinical picture: MPS type I (Hurler syndrome/Hurler-Scheie/Scheie syndrome), II (Hunter syndrome), III (Sanfilippo syndrome), IV (Morquio syndrome), VI (Maroteaux-Lamy syndrome), VII (Sly syndrome), IX [2]. The overall estimated incidence is 1 per in 25000 individuals, however, the incidence of each MPS type independently is much lower, on the order of 1 per in 100000 to 1 per in 200000 individuals [3]. Except for MPS type II or Hunter syndrome, which is an X-linked recessive, all of the phenotypes have an autosomal recessive hereditary pattern [3]. Table 1 presents the main genetic and metabolic features of MPS types [4]. The clinical manifestations vary, including short stature and skeletal deformities, hepatosplenomegaly, hernias, and coarse facial appearance, with each variety exhibiting a distinct involvement of the cardiovascular, respiratory, and central nervous system (CNS) [1]. In terms of neurologic impairment, symptoms vary extremely, both in frequency and severity, among different types of MPS and individuals with each type of disease. The central and peripheral nervous systems may both be impaired. The most frequent findings consistent with CNS involvement are mental retardation, hydrocephalus, progressive spasticity, seizures, cerebral infarction, ataxia, cervical cord compression and myelopathy, sleep apnea, optic atrophy, hearing impairment, hyperactivity with aggressive behavior [1]. Carpal and tarsal tunnel syndromes are the most common features of peripheral nervous system impairment [1]. Intellectual impairment is a prevalent feature in patients with MPS III and severe forms of MPS I, II, and VII, whereas normal cognition is retained in other types of the disease [1]. The cause of this heterogeneity is unknown, particularly because existing neuropathologic studies reveal neuron abnormalities even in patients in whose the CNS is not involved [1]. MPS is diagnosed based on quantitative analysis of GAGs levels in the patient's urine. Furthermore, an enzymatic study specific to the type of MPS and a molecular study is also performed [5]. The treatment of MPS is a complex process [5]. The development of enzyme replacement therapy (ERT) and possible new therapeutic regimens targeted at MPS neurologic manifestations highlighted the necessity to find accurate indicators for prognosticating outcomes and tracking CNS development. To avoid serious complications, CNS involvement must be detected early and monitored closely, rendering neuroimaging studies extremely important [1].

Aim of the Study

This study aims to describe the magnetic resonance imaging (MRI) findings of the brain and spine in patients with MSP and correlate them with the type of MPS and clinical severity, and finally to compare these findings with those previously published.

Materials and Methods

A retrospective evaluation was conducted of 12 brain and spine MRIs of patients (07 females and 06 males) who had been diagnosed and followed up with MPS from 2021 to this day in our radiology department. The initial diagnosis was performed by confirming high urinary GAG excretion and measuring the activity of the corresponding deficient enzyme. Whenever possible, a genetic study was also completed. We classified patients as having different types of MPS according to results from the above studies. In addition, patients may present severe or mild forms of MPS, with poorer or better prognoses, depending on the age at the onset of symptoms and the neurological course of the disease. The 12 patients under study were subdivided as follows: 07 with type I (05 had severe MPS or Hurler syndrome and 02 had moderate MPS or Hurler-Scheie syndrome); 02 with type II or Hunter syndrome (01 patients had a severe form and 1 had a moderate form), 1 type III or Sanfilippo; 1 type IV or Morquio syndrome; and 1 type VI or Maroteaux-Lamy syndrome. There were no cases of MPS type VII, or type IX. At the time of the MRI examinations, patient ages ranged between 05 and 14 years, with a mean age of 7.75 years. The imaging protocol of brain MRI included the standard sequences: sagittal T1, axial T2, axial T2 Flair, DWI (diffusion-weight-

Disease type		Deficient enzyme	Accumulated metabolites DMX	Radiographic and clinical findings							
				SS	CFF	OM	JS	CRD	CC	MR	
Type I (Hurler)	H	Alpha-L-iduronidase	hs, ds	+	+	+	+	+	+	+	+
	HS/S			Patient exhibits these findings moderate (HS)+/ mild(S)+							+/- !
Type II (Hunter) severe/mild		Iduronate sulfatase	hs, ds	++	+	+	+	+	+	--	++/-
Type III (Sanfilippo)	A	Heparan sulfamidase	hs	Patient exhibits these findings -/mild +						-	+~
	B	N-acetylglucosaminidase									
	C	Acetyl-CoA: alphaglucosaminide Acetyltransferase									
	D	N-acetylglucosamine 6-sulfatase									
Type IV (Morquio)	A	Galactose-6-sulfate sulfatase	ks, cs	+	+ #	-/+	-/+	+ *	+	+	- !
	B	Beta-galactosidase									
Type VI (Maroteaux-Lamy)		N-acetylgalactosamine4-sulfatase	ds	+	+	+	+	+	+	+	- !
Type VII (Sly)		Beta-glucuronidase	hs, ds, cs	+	+	-/+	+	+	+	+	-/+

Table 1: *Summary of the important features of the MPS types [1].*

H: Hurler; HS: Hurler-Schie; S: Schie; hs: Heparan Sulfate; ds: Dermatan Sulfate; ks: Keratan Sulfate; cs: Chondroitin Sulfate; DMX: Dysostosis Multiplex; SS: Short Stature (#: Evident Due to Platyspondyly); CFF: Coarse Facial Features; OM: Organomegaly (Hepatomegaly and/or Splenomegaly); JS: Joint Stiffness (: Stiffness and Laxity); CRD: Cardiorespiratory Disorders; CC: Corneal Clouding; MR: Mental Retardation [!: Patients Exhibit Normal Intelligence with MPS Type 1 S (Schei), Type IV, and Type VI]; ~: Mental retardation and/or Hyperactivity.*

ed imaging) and axial T2 EG (susceptibility-weighted imaging) and T1 3D post-contrast. The imaging protocol of spine MRI included the standard sequences: sagittal T1, T2, STIR, additional sequences are performed when scoliosis is present coronal T2 is performed or in the presence of sign of myelopathy axial T2 is also performed. Images were assessed by expert radiologists who were not informed about the patient's neurological conditions. For some of the cases, they were aware of the type of MPS in question. Of the 12 patients who underwent a brain MRI examination, 2 had two imaging tests during the follow-up period. The remaining patients underwent a single test, usually performed during the first month following the diagnosis or suspected diagnosis. Once patients were diagnosed, they were assessed clinically on a six-month or yearly basis by the appropriate pediatric sub-specialty (pediatric neurology, otorhinolaryngology, traumatology, cardiology, ophthalmology, etc).

Results

Brain MRI showed neuroimaging abnormalities in all patients in our series, except for one patient with Hurler-Scheie syndrome where brain MRI was normal. The most frequent findings in brain MRI were dilated Virchow-Robin perivascular spaces (n = 08/12, 20%), white matter abnormalities (n = 06/12, 15%), ventriculomegaly/hydrocephalus (n = 05/12, 12%), Cortical and subcortical cerebral atrophy (n

= 04/12, 10%, 2 with Hurler syndrome, 1 with 1 type IV or Morquio syndrome and 1 with type III or Sanfilippo syndrome), Posterior fossa abnormalities (n = 04/12, 10%), arachnoid cyst (n = 04/12, 10%), craniosynostosis (scaphocephaly n = 04/12, 10%). Three patients presented alterations of the posterior cranial fossa, including cerebellar hypoplasia in one patient with Hurler syndrome, and megacisterna magna in 3 children (1 with moderate Hunter syndrome and two others with Hurler syndrome). We found closed meningo-encephalocele associated with concave remodeling roof of the ethmoid in 02 patients with Hurler syndrome, bilateral optic nerve sheaths enlargement in 02 patients with MSP I (01 with Hurler syndrome and the other with Hurler-Scheie syndrome), morphological abnormality of sella turcica in one patient with Hurler-Scheie syndrome.

Spine MRI showed neuroimaging abnormalities in all patients, the most frequent findings: periodontoid soft-tissue thickening (n = 07/12; 20%; 3 with Hurler syndrome, 1 with Hurler-Scheie syndrome, 1 with severe Hunter syndrome, 1 with moderate Hunter syndrome, and 1 with Maroteaux-Lamy syndrome), spinal canal stenosis (n = 07/12; 20%), cord compression (n = 04/12; 11%) was detected in 3 patients at the cervical area, and 1 patient in the lumbar area, myelopathy (n = 02/12, 6%), Odontoid hypoplasia (n = 03/12; 8% in the patient with MPS VI and in 1 girl with Hurler-Scheie syndrome, and 1 boy with Hurler syndrome), morphological abnormality of vertebral bodies (n = 07/12; 20%). Other isolated findings: syringomyelia in 2 patient with Hurler syndrome, scoliosis in 1 patient with Hurler syndrome, and kyphosis in 2 patients one with Hurler syndrome and the other with MPS IV.

In cases with MPS I or II (the most frequent in our series), we found no link between neuroradiological changes and specific type of MPS, or between changes and disease severity (Table 2).

Patient	Syndrome	Age at MRI	PVSEs	WMSAs	Ventriculomegaly/ HC	CA	PFA	ONSE	Arachnoid cyst	Bone abnomalities
1	MSPI(H)	6	+	+	+	+	-	+	+	-Scaphocephaly -CRE
2	MSPI(H)	8	+	-	-	-	+ (MM)	-	-	-
3	MSPI(H)	5	+	-	+	-	-	-	+	Scaphocephaly
4	MSPI(H)	5	+	-	-	-	+ (MM)	-	-	CRE
5	MSPI(H)	6	-	+	+	+	+ (CH)	-	+	Scaphocephaly
6	MSPI(SH)	10	+	+	+	-	-	+	-	JSS
7	MSPI(SH)	14	-	-	-	-	-	-	-	-
8	MSPII(mo-de-rate)	11	-	+	-	-	+ (MM)	-	+	-
9	MSPII (severe)	5	+	+	-	+	-	-	-	Scaphocephaly
10	MSPIII	9	+	-	+	-	-	-	-	-
11	MSP IV	7	-	-	-	+	-	-	-	-
12	MSP VI	7	+	+	-	-	-	-	-	-

***Table 2**: Brain IMR findings from patients included in the study.*

MSP I(H): Hurler Syndrome; MSP I(SH): Hurler-Scheie Syndrome; PVSEs: Perivascular Space Enlargements; WMSAs: White Matter Signal Alterations; HC: Hydrocephalus; CA: Cerebral Atrophy; PFA: Posterior Fossa Abnomalities; ONSE: Optic Nerve Sheath Enlargement; MM: Mega Cisterna Magna; CH: Cerebellar Hypoplasia; CRE: Concave Remodeling Roof of the Ethmoide Bone (Those Patient have also Closed Meningo Encephalocele on this Level); JSS: J-Shaped Appearance of the Sella Turcica; -: Absent; +: Present.

Discussion

Magnetic resonance imaging (MRI) is the imaging modality to evaluate cerebral and spinal cord abnormalities in patients with MPS, as it is in patients with other metabolic disorders [3,6,7]. Patients who receive a diagnosis of MPS or who are suspected of having MPS should undergo an MRI of the entire neuraxis for complete evaluation because manifestations of this disease are not limited to the brain, the spine can also be affected as proven in our study. We must keep in consideration that many MPS patients require anesthesia before the examination, and there is a well-documented association in the literature between MPS and difficult airway management [8]. Therefore, the MRI protocol should be optimized to be as short as possible. A proposed protocol is summarized in table 3. Cranial and spinal MRI revealed a broad spectrum of changes in patients with MPS (Table 4 and 5 summarizes the main imaging findings in each type of MPS) [3]. The most prominent brain features, in almost all types of the disease, are Perivascular space (also called the Virchow–Robin space) enlargement (PVSE), white matter signal alterations (WMSAs), ventriculomegaly/hydrocephalus, and cerebral atrophy, while in spinal neuroimaging, canal stenosis, cord compression, and myelopathy are common findings [1].

Brain MRI
• 3D T2 weighted images reconstructed in axial, sagittal, and coronal planes • Sagittal T1 weighted image • Axial FLAIR • Axial gradient-recalled echo or susceptibility weighted imaging • Axial diffusion-weighted imaging with apparent diffusion coefficient mapping
Cervical, thoracic and lombosacral spine MRI
• Sagittal T1 weighted image • Sagittal T2 weighted image • Sagittal STIR • Coronal T2 weighted image • Axial T2 weighted image

Table 3: *Proposed MRI protocol for patients with MSP.*

Neuroimaging Finding	MRI appearance
Enlarged perivascular space	Cribriform or fusiform cystic lesions isointense to cerebrospinal fluid (CSF) at all sequences; diameters ranging from 2 mm to more than 8 mm
White matter signal alterations	Focal or confluent areas of T1 hypointensity and T2-FLAIR hyperintensity
Hydrocephalus	Dilatation of ventricular spaces typically associated with enlarged subarachnoid spaces
Cerebral atrophy	Enlargement of cortical sulci and fissures
Cervical spinal canal stenosis	Dysplastic odontoid process associated with soft-tissue mass, which is usually iso- or hypointense on T1-weighted images and hypointense on T2-weighted images, with or without spinal cord compression and myelopathy; functional imaging of the cervical spine may be necessary to better depict atlantoaxial instability
Bone abnormalities in the skull and spine	Whaped vertebral bodies, platyspondyly, anterior beaking with posterior scalloping of vertebral bodies (bullet-shaped vertebrae), intervertebral disk changes, gibbus deformity, scoliosis, odontoid dysplasia, thickening of the diploe, morphologic abnormalities of the sella turcica, and macrocephaly

Table 4: *Neuroimaging findings in MPS and MR imaging appearance [4].*

Type of MPS	Perivascular space enlargements	White matter signal alterations	Hydrocephalus	Cerebral atrophy	Spinal canal stenosis	Dysostosis multiplex
MPS I	Typical and pronounced	Typical and pronounced	Typical and pronounced	Typical and pronounced	Typical	Typical and pronounced
MPS II	Typical and pronounced	Typical and pronounced	Typical and pronounced	Typical and pronounced	Typical	Typical and pronounced
MPS III	Typical	Typical and pronounced	Typical	Typical and pronounced	Typical	Uncharacteristic
MPS IV	Uncharacteristic	Typical	Typical	Uncharacteristic	Typical and pronounced	Typical and pronounced
MPS VI	Typical	Typical	Typical	Typical	Typical and pronounced	Typical and pronounced
MPS VII	Uncharacteristic	Typical and pronounced	Uncharacteristic	Uncharacteristic	Typical	Typical and pronounced
MPS IX	Uncharacteristic	Uncharacteristic	Uncharacteristic	Uncharacteristic	Uncharacteristic	Uncharacteristic

Table 5: *Neuroimaging findings according to type of MPS [4].*

In our series, one of the most frequent abnormalities observed in cranial MRI was PVSEs (n = 8/12, 20%) (Figure 1 and 2). This common but non-specific feature can occur in other numerous diseases, but also in healthy people. The inferior parts of the basal ganglia, the centrum semiovale, and the midbrain are the area normally affected in the case of the MSP. Nonetheless, compared to healthy people, MPS patients have some gliotic foci around the enlarged perivascular spaces. PVSEs in MPS patients have been linked to GAGs storage around the perivascular areas or leptomeninges, resulting in a decrease in cerebrospinal fluid (CSF) absorption [3,4,9]. In the current study, PVSEs were usually located in the periventricular white matter and/or the corpus callosum [9,10], with diameters mostly < 8 mm. PVSEs were more common in patients with MPS I, II, and VI, and no correlation was found between these patients' age groups and the number of PVSEs. Although PVSEs was not found in the patient with MSP type III and the patient with type IV in this series (Table 2). Although PVSEs may not develop in some MPS patients, PVSEs should be considered as evidence for the diagnosis of MPS when accompanied by other specific imaging findings, especially when these are located in the corpus callosum [3]. A prior study comparing patients with MPS and cognitive decline to those with MPS without cognitive decline found no significant difference between the groups in the prevalence of enlarged perivascular spaces [11]. Enlarged PVS have been described so far in MPS I, II, III, and VI. In general, PVSEs were more profound in patients with MPS I and II, with a ‘‘sieve-like” appearance [1,12]. Cystic lesions are usually linear, varying from patchy to diffuse [1,9], and most commonly affect the periventricular white matter, followed by the corpus callosum (Figure 1), basal ganglia, subcortical white matter, thalamus, and brainstem [1], but all parts of the brain can be affected. The PVSEs range from 2 to 8 mm in diameter in most of the cases [1].

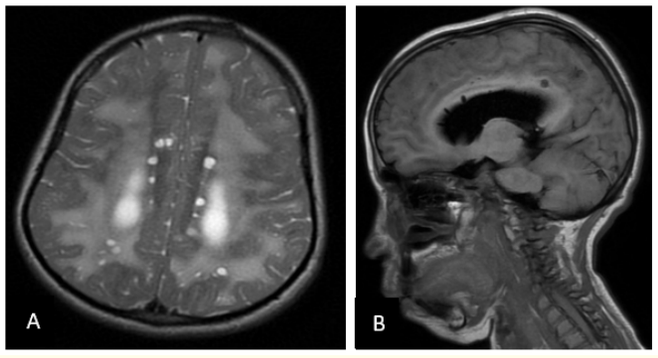

Figure 1: *MPS I and neurologic impairment in a 6-year-old boy. Axial T2(A) and sagittal T1 (B) MR image of the brain shows symmetric periventricular white matter lesions. There is associated cystlike dilated perivascular space enlargements in peri-ventricular level and in the body of the corpus callosum.*

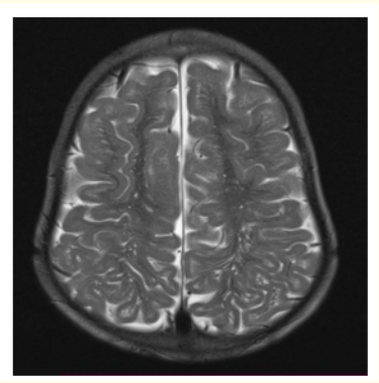

Figure 2: *MPS III and neurologic impairment in a 9-year-old boy. Axial T2 MR image of the brain shows perivascular space enlargements at the centrum semiovale level.*

The second most frequently encountered findings in this series was WMSAs, which varied in form (Patchy or diffuse) and severity in different types of disease (n = 6/12, 15%) (Figure 1, 3 and 4). These signal abnormalities are presumed to be a result of abnormal myelination and/or gliosis, and they reportedly increase as the disease progresses [4,13]. WMSAs were prominent in type I, and III of MPS in this series. The white matter regions affected were mainly the periventricular white matter areas, and subcortical white matter areas were also affected to a lesser extent. WMSAs are periventricular and diffuse in MSP type III, while in the other types of MSP, WMSAs are patchy [1,4]. The current series' results concurred with these findings. Although the relationship of patchy or diffuse cerebral WMSAs with clinical findings is a controversial issue in the literature, a positive association between the extent of white matter signal alterations and the duration of the disease has been reported [6].

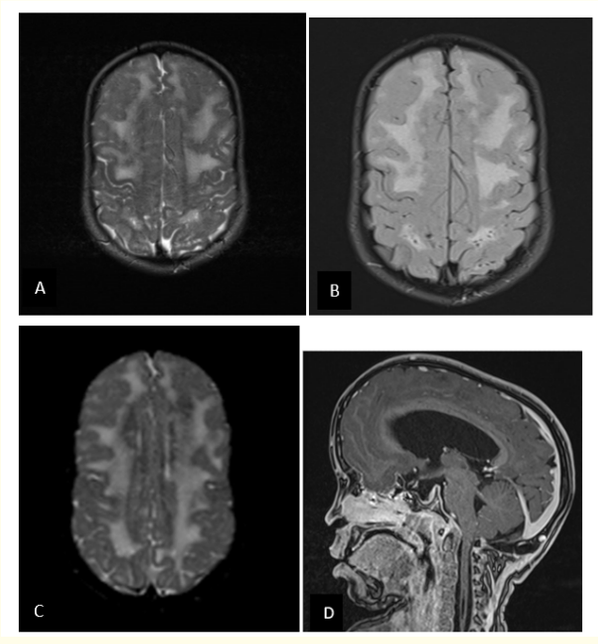

Figure 3: *MPS I in an 6-year-old girl. Axial T2 (A), FLAIR (B), diffusion (C) and sagittal post gadolinium (D) MR image of the brain shows abnormal high signal intensity in the periventricular and subcortical white matter, with associated hydrocephalus. Note : craniosynostosis with scaphocephaly.*

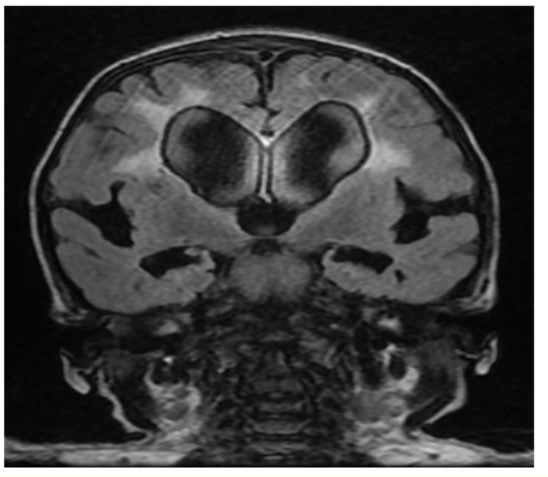

Figure 4: *MPS I and neurologic impairment in a 6 -year-old girl. Coronal FLAIR MR image of the brain shows symmetric periventricular white matter lesions. There is associated mild ventriculomegaly and discrete widening of the sylvian fissures.*

Hydrocephalus/ventriculomegaly (n = 5/12, 12%) (Figure 5), and cerebral atrophy (n = 4/12, 10%) (Figure 6) were the other two important and significant features in this series. These findings were especially prominent in type I, II, III, and IV patients [1,3,14] (Table 2). In some of the patients with both hydrocephalus and parenchymal atrophy, one of these findings (either hydrocephalus or parenchymal atrophy) was usually more prominent (Figure 12) [15]. There are currently suggested reasons for the mechanism of hydrocephalus development in MPS patients including the presence of abnormal CSF absorption and venous hypertension [1,3]. The meninges are affected as well, and the accumulation of GAGs at this level alters the function of the arachnoid granulations, decreasing CSF reabsorption, and the abnormal bone proliferation at the skull base decreases cerebral venous outflow, Communicating hydrocephalus results from one or both processes [4].

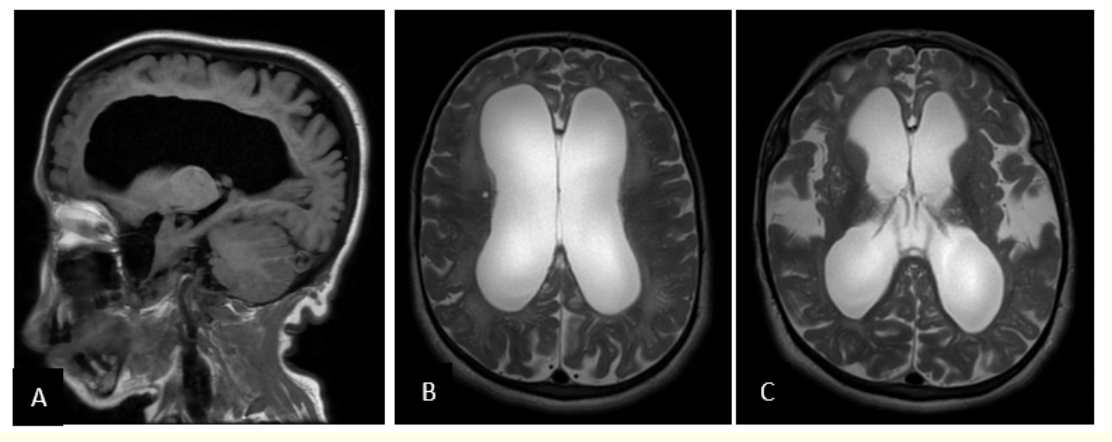

Figure 5: *Hurler syndrome in an 6-year-old boy. Sagittal T1 (A) and Axial T2 (B, C) MR image of the brain shows abnormal high signal intensity in the periventricular and subcortical white matter, with associated hydrocephalus. Note also the enlarged cortical sulci in the frontal lobe and the sylvian fissures.*

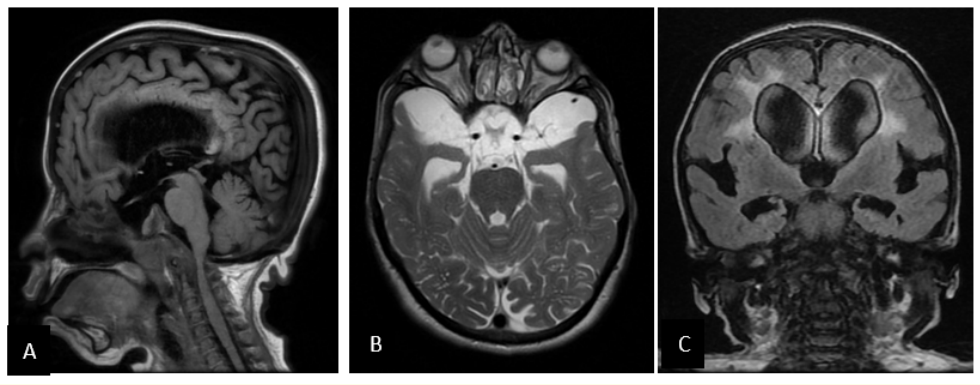

Figure 6: *MSP II and neurologic impairment in a 5-year-old girl, sagittal T1 (A), axial T2 (B) and coronal FLAIR (C) images, shows widening of the cortical sulci and sylvian fissures in relation to cerebral atrophy.*

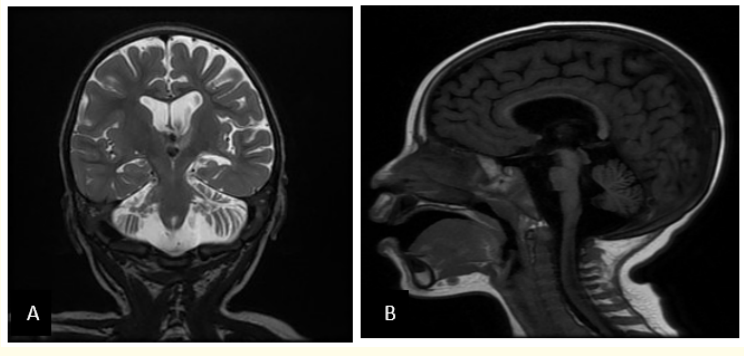

Figure 7: *Coronal T2-weighted (A) and midsagittal T1-weighted (B) MR images of a child with Hurler syndrome at the age of 6 years show cerebellar hypoplasia involving mostly the cerebellar hemisphere with secondary enlargement of the fourth ventricle.*

Patients in this series who present with MPS have also been described as having abnormal MRI features of the posterior cranial fossa. The most frequent finding in our series is mega cisterna magna (n = 3/12) (Figure 8), which is frequent in patients with MPS II [1,3,12], and has been also reported in MPS I and IIIB [12]. Arachnoid cyst, which can develop in both the posterior fossa and the supratentorial compartment, remains the main differential diagnosis [1,4]. The causes of posterior fossa arachnoid cysts and mega cisterna magna are unclear, but the most common theories include splitting or duplication of the arachnoid matter, brain structure agenesis, and disturbances of CSF circulation [1]. We observed cerebellar hypoplasia affecting mostly the cerebellar hemisphere in one patient with Hurler syndrome (Figure 4). Cerebellar hypoplasia is an uncommon finding in MPS and was previously reported in MPSI and MSP II [16,17].

Other findings include arachnoid cyst (n = 3/12, 10%). This can be attributed to the deposition of glycosaminoglycans in the meninges, which interferes with the circulation of CSF [3,10,14,18,19,29]. Arachnoid cysts were found in patients with MSP I [20], MSP II [3], MSP III [21], MPS IV [18], and MSP VI [22]. Arachnoid cysts from meningeal deposition of GAGs are classically seen at the anterior temporal poles [18].

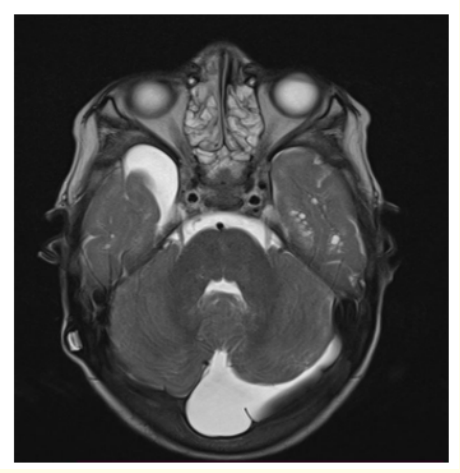

Figure 8: *MPS II and neurologic impairment in a 11-year-old girl. Coronal T2 MR image of the brain schows a mega citerna magna of the posterior fossa. Right temporal arachnoid cyst is also observed.*

One finding rarely reported was optic nerve sheath enlargement found in 2 patients (Figure 11). It has been reported to be associated with MPS. Widening of the optic nerve and its sheath was one of the sonographic abnormalities seen in patients with MSP type I, II, and VI MPS in a prior ophthalmology study. Optic nerve sheath enlargement was thought to be due to increased intracranial hypertension or meningeal GAGs storage [3,22]. The communicating hydrocephalus may also be related to this finding [3,4]. Widening of the CSF space in the optic nerve sheath may contribute to progressive pseudoexophthalmos, and can cause optic nerve atrophy, which is a common complication in patients with MSP I [1,10,23].

In the cranial MRI evaluations of the present study, the most frequent bone abnormality was the concave remodeling of the roof of the ethmoid, resulting in closed meningoencephaloceles (Figure 9 and 12) in 2 patients with Hurler syndrome. This uncommon finding was previously reported in MPSI [3,24], MSP II [4,25], and MSP VI [4].

Figure 9: *MPS I and neurologic impairment in a 5-year-old girl with Hurler syndrome. Coronal T2 MR image of the brain schows a concave remodeling roof of the ethmoide bone. This associated with closed meningo encephalocele on this level.*

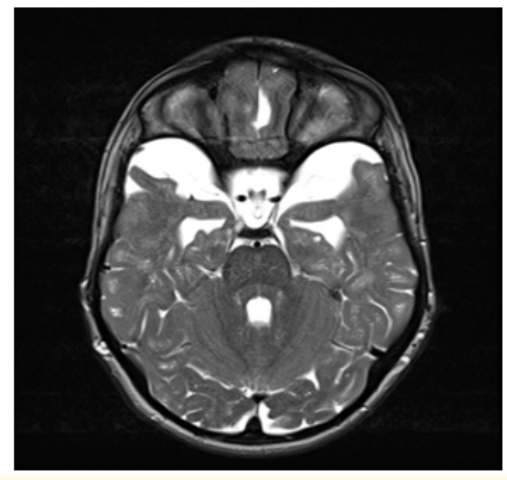

Figure 10: *MPS I and neurologic impairment in a 6-year-old boy with Hurler syndrome. Axial T2 MR image of the brain shows bilateral anterior temporal arachnoid cyst.*

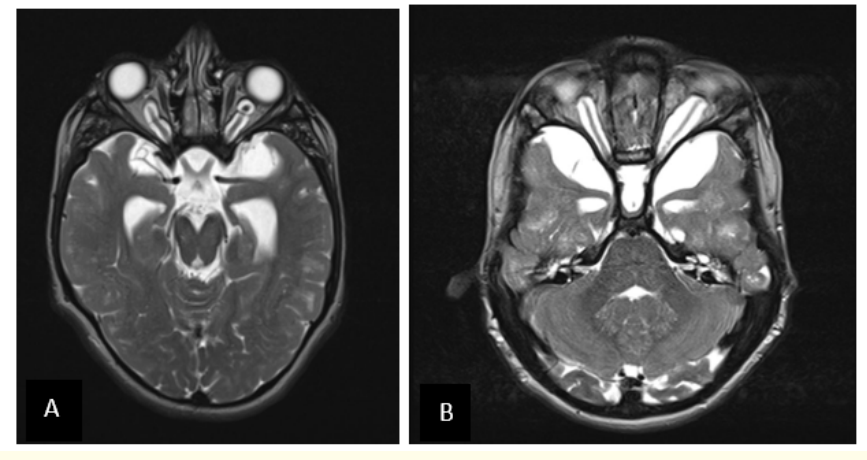

Figure 11: *MPS I and neurologic impairment in a 6-year-old boy with Hurler syndrome (A) and 10-year-old(B) with Hurler-Sheie syndrome. Axial T2 MR image of the brain shows bilateral optic nerve sheath enlargement.*

Other findings include the J-shaped appearance of the sella turcica (JSS) found in 1 patient with MSP I. This nonspecific finding may be considered a normal variant in healthy individuals but it may also be a sign of certain disease processes, for instance, chronic hydrocephalus, optic glioma, osteogenesis imperfecta, achondroplasia, neurofibromatosis, and MPS [4]. JSS has been reported in MSP type I, II, IIIA, IV, and VI, and it is usually associated with growth hormone deficiency [1,4].

We found no correlations between the type of MPS or the severity of its clinical form and brain MRI findings. 1 of the 2 patients with Hurler-Scheie syndrome didn't show WMSAs, and this was also true of 3 of the 5 patients with Hurler syndrome. We observed an in-

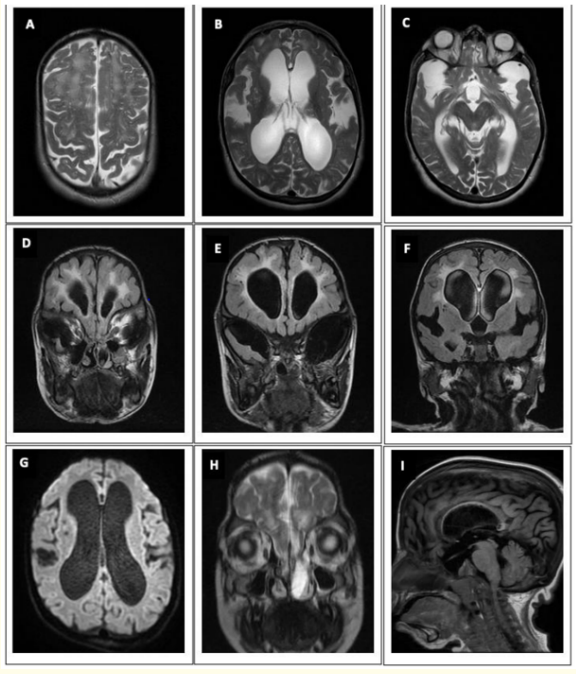

Figure 12: *Hurler syndrome and neurologic impairment in a 6-year-old boy. T1, T2, FLAIR MRI imgaes shows. Note the hyperintense signals in T2 and Flair on the supratentorial white matter (A, D-F) and marked dilation of perivascular Virchow-Robin spaces (A). Associated with this is moderate triventricular dilatation (B, E-G), cortical sulci in the parieto-temporal lobe and extensive widening of the sylvian fissures (B-F), closed meningoencephalocele (D), and temporal arachnoid cysts (C).*

crease in PVS in 1 patient with severe Hunter syndrome. This means that the brain alterations described in our patients (increase in PVS, WMSAs, hydrocephalus, etc.) may be independent of the severity of the condition, our study joins that of M.L. Calleja Gero and al [5]. However, other studies point to a direct link between the extent of these neuroradiological changes and the severity of the disease [12]. Some studies in particular found a correlation between the cognitive level and WMSAs (but not with other neuroimaging changes) [24].

In our series, one of the most frequent abnormalities observed in spine MRI was periodontoid soft-tissue thickening (n = 7 /12, 20%) (Figure 14, 16 and 17) and spinal canal stenosis (n = 7/12) with (Figure 14 and 16) or without (Figure 17) signs of compressive myelopathy. These findings are not rare in patients with MPS and might even be the first sign leading to disease diagnosis [1,25]. It represents a prominent finding in MPS IV, VI, and I, and cases of MPS II, IIIA, and VII have also been reported [1,2,9,12,14,25-27]. It can affect many levels of the spinal cord, but the craniocervical junction (Figure 14) [1,28], and thoracolumbar spine are the most affected levels (Figure 16) [1, 29] as in the case of our patients. Compression of the spinal cord at the thoraco-lumbar level is secondary to a kyphosis which is due to the deformation of a vertebra which causes a narrowing of the spinal canal [29] (Figure 16). Spinal cord compression appears to be multifactorial. However, there are 2 main proposed physiopathologic mechanisms. The first occurs with GAG deposition and infiltration of surrounding tissues and particularly the dura mater by a soft-tissue mass. On T1-weighted images, this mass is usually iso or hypointense, and hypointense on T2-weighted images. MPS IV, VI, and I show a high propensity for dural thickening, while this finding has been described to a lesser extent in patients with MPS II. The second mechanism suggests vertebral anomalies leading to deformities and atlantoaxial instability due to dysfunction of the odontoid process as etiopathology mechanisms for cord compression [1,18,25,29].

MRI is used to assess the nervous complications of MPS spinal involvement, it shows abnormal signal intensity at the level of myelopathy [1,29]. The signs and symptoms of myelopathy may not be related to the degree of spinal cord compression, since the neurologic deficit is usually milder than suggested by MR imaging [18,25].

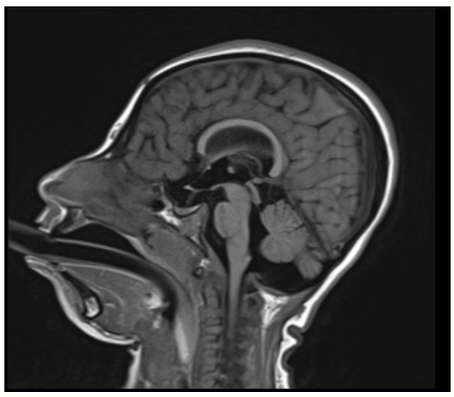

Figure 13: *MSP I and bone abnormality in a 14-year-old girl with Hurler-scheie syndrome, shows J-shaped appearance of the sella turcica.*

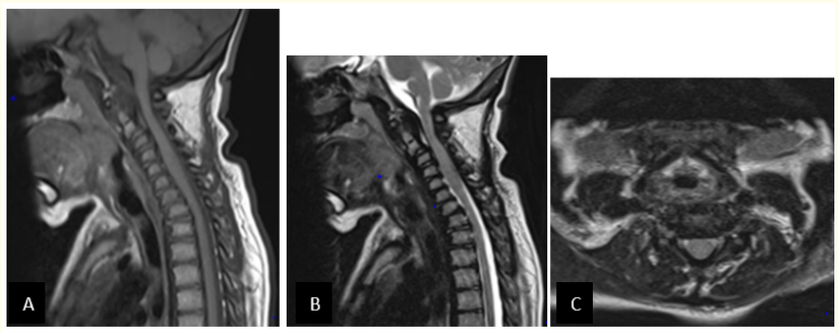

Figure 14: *MSPI Spine impairment in a 8-year-old GIRL with Huler syndrome. Sagittal T1 (A) and T2 (B), axial T2 (C) MR images shows spinal cervical canal stenosis due to periodontoid theckining With reduced sub-arachnoid spaces with cord compression at the level of C1-C2 and C3-C4 with mylopathy at the level of C 4-C4. Note: Odontoid hypoplasia.*

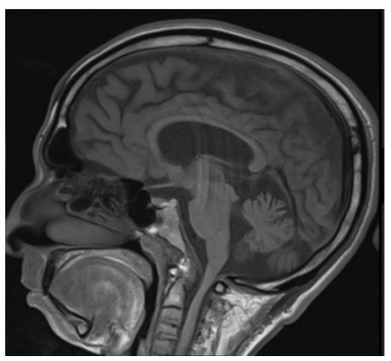

Figure 15: *Sagittal T1 MR images: Odontoid hypoplasia.*

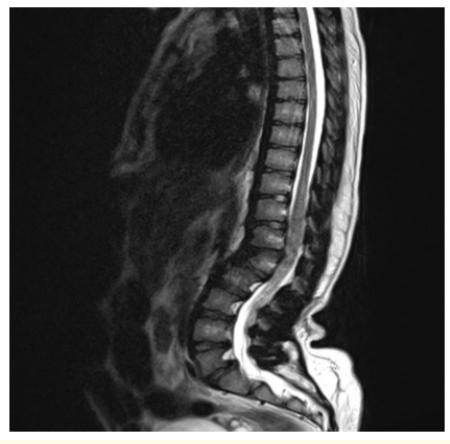

Figure 16: *MSP VI spine impairment in a 11-year-old girl. Sagittal T2 MR images shows typical platyspondylia of L1 vertebra with typical kyphosis thoracolumbar, with associated thoracolumbar stenosis at this level with myelopathy.*

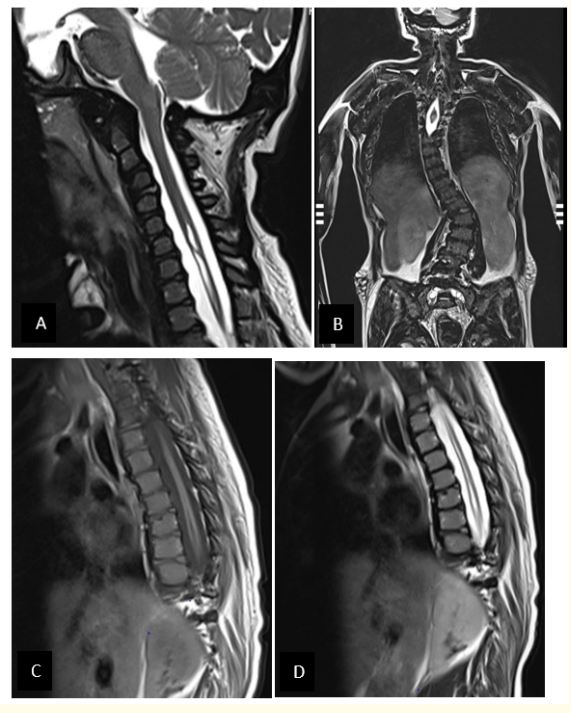

Figure 17: *MSPI Spine impairment in a 11-year-old boy with Huler syndrome. Sagittal T2 (A, D), sagittal T1 (C), coronal T2 (B) MR images shows spinal cervical canal stenosis due to periodontoid theckining reducing the sub-arachnoid spaces without cord compression, associated with typical platyspondylia of C4, C5 vertebra with typical kyphosis thoracolumbar. A cervico-dorso-lumbar syringomyelia and Odontoid hypoplasia are also observed. Note the double curvature dorso-lumbar scoliosis.*

In the spine MRI of the present series, the most frequent bone abnormality found was platyspondyly (n = 7/12, 20%) (Figure 14, 16 and 17). Dysostosis multiplex is one of the most common manifestations of MPS, and patients show different degrees of bone and joint involvement, mostly as a result of GAG deposition and abnormal bone maturation [25,30]. Given this, spine MRI shows a serve abnormalities involving the vertebral bodies and inter-somatic disks. Characteristic features are platyspondyly, bullet shape, and breaking of vertebrae, while disks were reported to be dehydrated [1,25,31,32].

The second most findings was Odontoid hypoplasia in 3 patients 2 with Hurler syndrome (Figure 14 and 17), and the other with MPS IV (Figure 15). Odontoid abnormalities have mostly been reported in patients with MPS IV, VI, and I, and can range from complete aplasia to different degrees of hypoplasia [1,25].

Another uncommon finding was found, syringomyelia in 2 patients with Hurler syndrome (Figure 17). This finding is rarely reported in the literature, Hite., *et al*. [33] described the case of a patient with Maroteaux-Lamy who developed holo-cord syringomyelia. In another case description, signal-intensity changes within the cervical cord were demonstrated, but the authors were unable to determine whether this finding corresponded to GAGs storage or demyelination [1,32].

In total, these abnormalities, whether at the brain or spine can be present or absent and occur in different combinations and severities, even in individuals with the same MPS type [18,34] as proved by our series.

Our series has obvious limitations. First, it was a retrospective study and most of these patients had only one MRI evaluation and some were lost during follow-up. Thus, there are no specific treatment-related changes in the above-mentioned findings. Additionally, because of the small number of study subjects, our findings are mostly descriptive. Second, the ages at which brain MRIs were performed are heterogeneous. Finally, some of the MPS subtypes were not included and a comparison of the features could not be performed. A much larger sample would be requested to compare and obtain more reliable results.

Conclusion

The present series of 12 patients illustrates the typical MRI features of the brain and spine with MPS. With the recent advances in therapeutic interventions and prolonged life expectancy in MPS patients, for radiologists, especially neuroradiologists, it is important to be familiar with the main CNS manifestations of MPS.

Conflict of Interest

The author(s) declared no potential conflicts of interest with respect to the research, authorship, and/or publication of this article.

Funding Support

The author(s) received no financial support for the research, authorship and/or publication of this article.

Bibliography

1. Zafeiriou DI., *et al*. "Brain and spinal MR imaging findings in mucopolysaccharidoses: a review". *American Journal of Neuroradiology* 34.1 (2013): 5-13.

2. Lins CF., *et al*. "MRI findings of the cervical spine in patients with mucopolysaccharidosis type VI: relationship with neurological physical examination". *Clinical Radiology* 75.6 (2020): 441-447.

3. Reichert R., *et al*. "Neuroimaging findings in patients with mucopolysaccharidosis: what you really need to know". *Radiographics* 36.5 (2016): 1448-1462.

4. Damar Ç., *et al*. "Posterior fossa horns; a new calvarial finding of mucopolysaccharidoses with well-known cranial MRI features". *Turkish Journal of Medical Sciences* 50.4 (2020): 1048-1061.

5. GeroM LC., *et al*. "Neuroimaging findings in patient series with mucopolysaccharidosis". *Neurología* 27.7 (2012): 407-413.

6. Vedolin L., *et al*. "Brain MRI in mucopolysaccharidosis: effect of aging and correlation with biochemical findings". *Neurology* 69.9 (2007): 917-924.

7. Cheon JE, *et al*. "Leukodystrophy in children: a pictorial review of MR imaging features". *Radiographics* 22.3 (2002): 461-476.

8. Kirkpatrick K., *et al*. "Mucopolysaccharidosis type I (Hurler syndrome) and anesthesia: the impact of bone marrow transplantation, enzyme replacement therapy, and fiberoptic intubation on airway management". *Pediatric Anesthesia* 22.8 (2012): 745-751.

9. Matheus MG., *et al*. "Brain MRI findings in patients with mucopolysaccharidosis types I and II and mild clinical presentation". *Neuroradiology* 46 (2004): 666-672.

10. Machnikowska-Sokołowska M., *et al*. "Mucopolysaccharidosis Type 1 among Children-Neuroradiological Perspective Based on Single Centre Experience and Literature Review". *Metabolites* 13.2 (2023): 209.

11. Gabrielli O., *et al*. "Correlation between cerebral MRI abnormalities and mental retardation in patients with mucopolysaccharidoses". *American Journal of Medical Genetics Part A* 125.3 (2004): 224-231.

12. Seto T., *et al*. "Brain magnetic resonance imaging in 23 patients with mucopolysaccharidoses and the effect of bone marrow transplantation". *Annals of Neurology: Official Journal of the American Neurological Association and the Child Neurology Society* 50.1 (2001): 79-92.

13. Manara R., *et al*. "Brain and spine MRI features of Hunter disease: frequency, natural evolution and response to therapy". *Journal of Inherited Metabolic Disease: Official Journal of the Society for the Study of Inborn Errors of Metabolism* 34.3 (2011): 763-780.

14. Ramos-Villegas Y., *et al*. "Neuroradiological Characteristics in Patients with Mucopolysaccharidosis Type II: A Systematic Review". *Journal of Medical Academics* 5.1-2 (2022): 13.

15. Matsubara Y., *et al*. "Cerebral magnetic resonance findings during enzyme replacement therapy in mucopolysaccharidosis". *Pediatric Radiology* 47 (2017): 1659-1669.

16. Alqahtani E., *et al*. "Mucopolysaccharidoses type I and II: new neuroimaging findings in the cerebellum". *European Journal of Paediatric Neurology* 18.2 (2014): 211-217.

17. Reichert R., *et al*. "Magnetic resonance imaging findings of the posterior fossa in 47 patients with mucopolysaccharidoses: A cross-sectional analysis". *JIMD Reports* 60.1 (2021): 32-41.

18. Rasalkar, D., *et al*. "Pictorial review of mucopolysaccharidosis with emphasis on MRI features of brain and spine". *The British Journal of Radiology* 84.1001 (2011): 469-477.

19. Palmucci S., *et al*. "Imaging findings of mucopolysaccharidoses: a pictorial review". *Insights into Imaging* 4.4 (2013): 443-459.

20. Friedmann I., *et al*. "Histopathological studies of the temporal bones in Hurler's disease [mucopolysaccharidosis (MPS) IH]". *The Journal of Laryngology and Otology* 99.1 (1985): 29-42.

21. Petitti N., *et al*. "Mucopolysaccharidosis III (Sanfilippo syndrome) type B: cranial imaging in two cases". *Journal of Computer Assisted Tomography* 21.6 (1997): 897-899.

22. Nicolas-Jilwan M., *et al*. "Mucopolysaccharidoses: overview of neuroimaging manifestations". *Pediatric Radiology* 48 (2018): 1503-1520.

23. Ashworth Jane L., *et al*. "The ocular features of the mucopolysaccharidoses". *Eye* 20.5 (2006): 553-563.

24. González A., *et al*. "Encephalocele in a patient with Hurler syndrome: description and therapeutic alternatives review". *Acta de Otorrinolaringología and Cirugía de Cabeza y Cuello* 50.1 (2022): 73-76.

25. Manara R., *et al*. "Closed Meningo (encephalo) cele: a new feature in Hunter syndrome*". American Journal of Neuroradiology 33*.5 (2012): 873-877.

26. Nakaoka S., *et al*. "Mucolipidosis II and III with neurological symptoms due to spinal cord compression". *Brain and Development* 43.8 (2021): 867-872.

27. SolankiG A., *et al*. "Cervical cord compression in mucopolysaccharidosis VI (MPS VI): Findings from the MPS VI Clinical Surveillance Program (CSP)". *Molecular Genetics and Metabolism* 118.4 (2016): 310-318.

28. Almeida JV., *et al*. "Spinal cord occupation ratio (SCOR) and its application in the diagnosis of cervical spinal cord compression in Mucopolysaccharidoses". *Journal of Inborn Errors of Metabolism and Screening* 10 (2022).

29. Crostelli M., *et al*. "Spine challenges in mucopolysaccharidosis". *International Orthopaedics* 43 (2019): 159-167.

30. Wilson S., *et al*. "Glycosaminoglycan-mediated loss of cathepsin K collagenolytic activity in MPS I contributes to osteoclast and growth plate abnormalities". *The American Journal of Pathology* 175.5 (2009): 2053-2062.

31. Kulkarni MV., *et al*. "Magnetic resonance imaging in the diagnosis of the cranio-cervical manifestations of the mucopolysaccharidoses". *Magnetic Resonance Imaging* 5.5 (1987): 317-323.

32. Parsons VJ., *et al*. "Magnetic resonance imaging of the brain, neck and cervical spine in mild Hunter's syndrome (mucopolysaccharidoses type II)". *Clinical Radiology* 51.10 (1996): 719-723.

33. Hite SH., *et al*. "Syringomyelia in mucopolysaccharidosis type VI (Maroteaux-Lamy syndrome): imaging findings following bone marrow transplantation". *Pediatric Radiology* 27 (1997): 736-738.

34. Rezayi A., *et al*. "An uncommon presentation of mucopolysaccharidosis type IIIb". *Iranian Journal of Child Neurology* 13.3 (2019): 105.

Volume 15 Issue 4 April 2023